Workspace Optimization of 3-Legged UPU and UPS Parallel Platforms With Joint Constraints

Mircea Badescu
Caltech Postdoctoral Scholar, Mem. ASME
e-mail: mircea.badescu@jpl.nasa.gov

Constantinos Mavroidis
Associate Professor, Mem. ASME
e-mail: mavro@coe.neu.edu

Robotics and Mechatronics Laboratory,
Department of Mechanical and Industrial Engineering,
Northeastern University,
Boston, MA 02115

In this paper the workspace optimization of 3-legged translational UPU and orientational UPS parallel platforms under joint constraints is performed. The workspace of both platforms is parametrized using several design parameters that span a large range of values. In this paper both the unconstrained and the constrained workspaces (i.e., workspace with joint limits) are used. For the workspace of each design configuration three performance indices are calculated using a Monte Carlo method: a) the workspace volume; b) the average of the inverse of the condition number and c) a Global Condition Index which is a combination of the other indices. Plots of each performance index as a function of the design parameters are generated and optimal values for these design parameters are determined. For the optimal design, it is shown that by introducing joint limits, the global isotropy of the parallel platforms is improved at the cost of workspace reduction. [DOI: 10.1115/1.1667922]

1 Introduction

In recent years, modular robots were increasingly proposed as means to develop reconfigurable and self-repairable robotic systems [1]. To perform impromptu custom tasks, increase the payload to weight ratio, and, in cases of emergency, self-repair, future inter-planetary robots and manipulation systems need to incorporate modularity and self-reconfiguration capabilities. Modular robots utilize many autonomous units, or modules, that can be reconfigured into a vast number of designs. Ideally, the modules will be homogeneous, small, and self-contained. The robot can change from one configuration to another by manual reassembly, or by itself. Self-reconfiguring robots adapt to a new environment or function by changing shape. Modules must interact with one another and cooperate in order to realize self-reconfiguration. Also, modular robots can repair themselves by removing and replacing failed modules. Since one self-reconfigurable modular robot can provide the functionality of many traditional mechanisms, they will be especially suited for space and planetary exploration, where payload mass must be kept minimum. Because they promise self-reparability and virtually limitless functionality, future self-reconfigurable modular robots are expected to be cheaper and more useful than current robot mechanisms in space missions.

In this project we investigate the use of 3-legged parallel platforms as joint modules of reconfigurable robots. Parallel platforms are currently being used in many applications as multi-degree of freedom systems with high rigidity, high payload to weight ratio, high precision and low inertia [2,3]. These properties are also desired characteristics for the joint modules of reconfigurable robots. Six-legged, six degrees-of-freedom (DOF) parallel platforms have been used as joint modules of reconfigurable robots in [4]. However, the high number of DOF and of actively controlled joints per module increases complexity and cost. In addition, a purely 3 DOF translational or spherical motion would require activation of all six module legs which means increase in energy consumption. Lately, a special type of 3-legged parallel platforms [6] has received a lot of attention because of its simple design and its pure 3-DOF translational motion with constant orientation. This platform could be combined with 3-legged, 3 DOF parallel platforms modules with purely spherical motion so that they form hybrid kinematic chains with decoupled translation and orientation [5]. Figure 1 shows an example of such a hybrid system. In this example a 2-arm reconfigurable robotic system is formed from a sequence of 3 DOF translational and orientational parallel platform modules.

The 3-DOF translational parallel platform that is studied in this paper was first proposed by Tsai [6] and was later on generalized by Di Gregorio and Parenti-Castelli [7,8]. It is made out of two equilateral triangular plates connected at the corners with three identical legs, as it is shown in Fig. 2. The legs are linked to the plates with universal joints. Linear actuators control the length of the legs forming prismatic joints. Due to the existence of universal and prismatic joints at each one of the legs, it is also called 3-UPU platform. By properly orienting the axes of universal joints, the moving plate can have only translational motion. The direct and inverse kinematics of this platform have been studied in [6,7,9]. Its static and singularity analyses have been performed in [8,10].

The workspace of parallel platforms in general has been studied thoroughly [3,11]. For the 3-UPU platform, the isotropy and workspace analyses have been performed in [9]. In that work, no constraints were assumed for the leg prismatic and universal joints, which means that full rotation of the universal joints and full extension of the prismatic joints, were considered. The workspace optimization was performed using one design parameter, which is the difference between the distances from the center to the corner of the triangular base and moving plates. Using a Monte Carlo method and varying the normalized lengths of the legs from 0 to 1 an optimum design is obtained at the value of 0.37 for the design parameter. However, from the practical point of view, universal joints have angular limitations that will reduce the workspace of the 3-UPU platform. Also, if these platforms are used as modules for a reconfigurable robot, they must be stacked, one on the top of the other, severely limiting their prismatic actuator stroke. From a design standpoint, universal and prismatic joint constraints should be included to produce a viable reconfigurable robot joint module. Moreover, the legs interference was not considered in the above mentioned work.

Different types of spherical or orientational parallel platforms have been proposed and analyzed. Merlet described several types of 2 and 3 DOF parallel platforms that can be used as wrists/orientation mechanisms [3]. Tsai classified the parallel platforms with rotational DOF in spherical and spatial orientation mechanisms [2,12]. All the moving points of a spherical parallel platform move on concentric spheres. Analysis and fabrication of a spherical 3 DOF platform were presented in [13]. Optimization of

Contributed by the Mechanisms and Robotics Committee for publication in the JOURNAL OF MECHANICAL DESIGN. Manuscript received Sept. 2002; revised July 2003. Associate Editor: M. Raghavan.

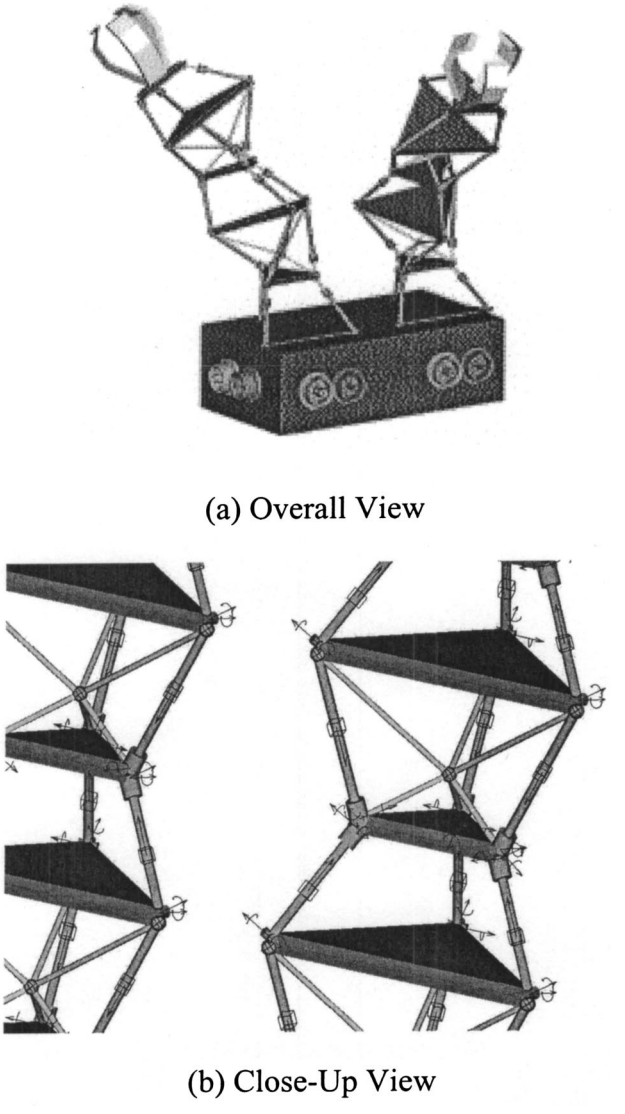

Fig. 1 Two-arm reconfigurable robot with 3-DOF parallel platform modules

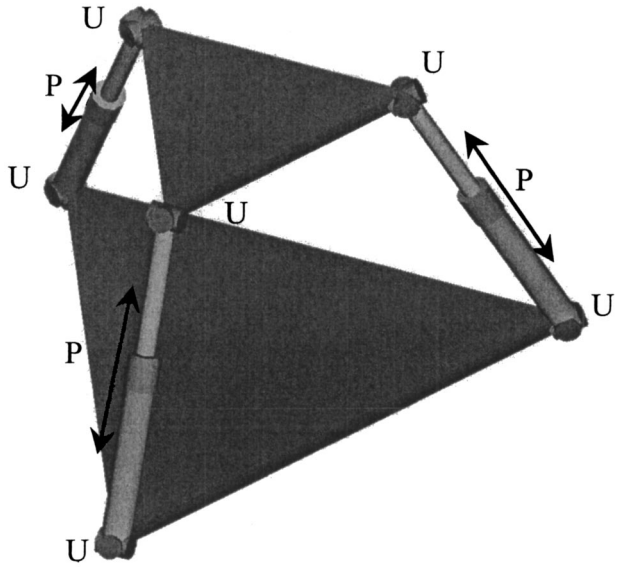

Fig. 2 The 3-UPU parallel platform

a spherical five bar parallel linkage was done in [14]. Gosselin and Angeles used three design criteria, symmetry, workspace volume and isotropy, to optimize a 3 DOF spherical platform [15].

The 3-DOF orientational platform that is studied in this paper is composed of two tetrahedrons with unequal equilateral triangular bases (Fig. 3) and three identical legs. The moving tetrahedron has a smaller triangular base than the fixed tetrahedron. The two tetrahedrons are connected at their tips using a spherical joint that determines the point around which the moving tetrahedron rotates. The corners of the two triangular bases are linked using three identical legs that are connected to the moving platform with universal joints and to the fixed platform with spherical joints. Linear actuators control the length of the legs forming a prismatic joint. Even though the points of the moving tetrahedron move on a sphere, due to the dissimilar motion of the legs the platform cannot be called spherical [2]. The kinematics and the singularity analysis of this platform were reported in [16,2]. To the author's knowledge, no workspace analysis, design optimization, or isotropy analysis have been performed yet for this 3-UPS platform.

In order to facilitate the development and motion planning of self-reconfigurable robots with parallel platforms as modules, the robot modules need to have similar motion and force capabilities at any one of their two ends (fixed and moving). This means that the platform modules should have similar type of motions and be able to apply the same forces regardless of which end is used as the fixed base or the moving component. Of the various types of spherical/orientational platforms that have been proposed so far, the 3-UPS parallel platform has this motion and force equivalence of its two ends. Therefore, this platform has been selected for further study in this paper.

In this paper the workspace optimization of translational 3-UPU and orientational 3-UPS parallel platforms with prismatic and universal joint constraints, and legs interference is performed. For the 3-UPU translational platform the workspace is parameterized using two design parameters, which are the prismatic joint stroke and the difference between the distances of the center to the corners of the triangular base and moving plates. For a large range of values for these design parameters the workspace of the corresponding 3-UPU platforms is calculated. This workspace is called in this paper the constrained workspace to distinguish it from the

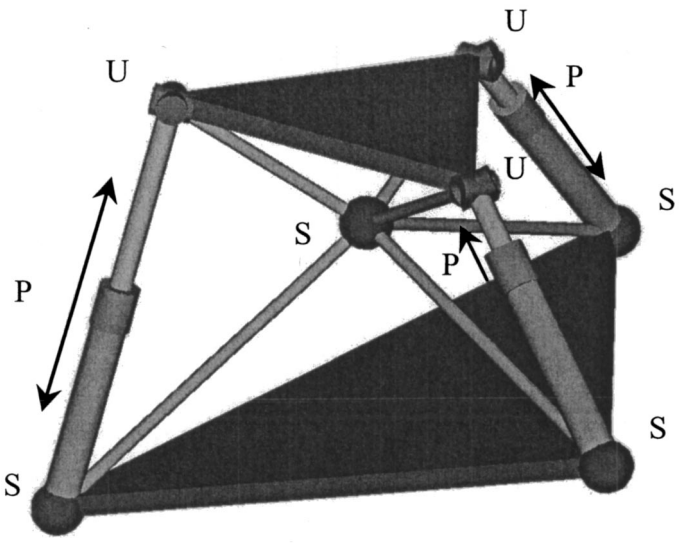

Fig. 3 The 3-UPS parallel platform

unconstrained workspace where no joint constraints are considered. For the constrained workspace of each design three performance indices are calculated: a) the workspace volume; b) the average of the inverse of the condition number and c) a Global Condition Index which is a combination of the other two performance indices. Plots of each performance index as a function of the two design parameters are generated and optimal solutions for these design parameters are identified. Finally, for the optimal design, it is shown that by introducing limits to the angles of the universal joints axes, the global isotropy of the parallel platform is improved. In this paper, global isotropy of a parallel platform or simply the isotropy of a parallel platform is called the average of the condition number of the Jacobian over the workspace.

For the 3-UPS orientational platform the workspace is parameterized using four design parameters, which are the prismatic joint stroke, the difference between the distances of the center to one of the corners of the triangular plate of the base and of the moving platform, the height of the platform in zero orientation, and the ratio of the heights of the two tetrahedrons. In a similar way as with the 3-UPU platform both the constrained and unconstrained workspaces are calculated and the same three performance indices are calculated. For determining the optimal design a Genetic Algorithm was implemented. The Global Condition Index was chosen as the objective function for optimization. The optimization was performed with and without imposing joint constraints. Plots of the 3-D workspace of the optimal designs are generated. Finally, for the optimal design, it is shown that by introducing limits to the angles of the universal and spherical joints, the isotropy of the parallel platform is improved. Moreover, the leg interference is taken into account and it is shown that the optimal design parameters are changed.

2 Mathematical Tools

In this section we present the mathematical/kinematic tools that were used to formulate the workspace optimization problems. These tools include the direct and inverse kinematics, the platforms' Jacobian matrices, their condition number and the Global Condition Index. For the direct and inverse kinematics and for the calculation of the Jacobian matrices we used the solution methodology proposed in [2,6]. For the Global Condition Index we used the same definition as in [9].

2.1 3-UPU Translational Platform. The 3-UPU parallel platform consists of a base plate, a moving plate and three identical limbs (see Fig. 2). The plates have equilateral triangular shape of different sizes. The limbs are connected to the plates with 2-DOF universal joints. A linear actuator controls the leg length, and forms a prismatic joint. Each universal joint is treated as two revolute joints with axes perpendicular to each other and intersecting at a point. In Fig. 4, u_{i1}, u_{i2}, u_{i4}, and u_{i5} are the unit vectors along the axes of the universal joints and u_{i3} is the unit vector along the prismatic joint axis for leg *i*. Tsai showed that by having u_{i1} parallel to u_{i5} and u_{i2} parallel to u_{i4} for each leg, then the moving plate would achieve pure translation in three dimensions [6].

As seen in Fig. 4, the position vectors of points A_i and B_i with respect to frames *A* and *B* respectively, can be written as:

$$^{A}\mathbf{a}_i=[a_{ix},a_{iy},0]^T, \quad \text{and} \quad ^{B}\mathbf{b}_i=[b_{ix},b_{iy},0]^T \tag{1}$$

Frames *A* and *B* are defined at the base and moving triangles respectively. Their origin is placed at the corresponding triangle's center. Their *z*-axis is perpendicular to each triangle's plane and their *x* and *y*-axes are in the triangle's plane. Parameter q_i denotes the length of leg *i*. Subscript *i* denotes one of the legs and can take the values 1, 2 or 3. Vector $\mathbf{c}_i$ is defined as the difference of $\mathbf{a}_i$ and $\mathbf{b}_i$. Letters in bold represent three-dimensional vectors. Superscript *A* or *B* on the left of a vector denotes the reference frame where its coordinates are calculated. Superscript *T* on the right of a vector denotes the transpose of a vector. Since vectors $\mathbf{a}_i$ and $\mathbf{b}_i$ are constants, vectors $\mathbf{c}_i$ are a constant too. Vector $\mathbf{e}$ determines the position of the center of the moving plate in the base coordinate system:

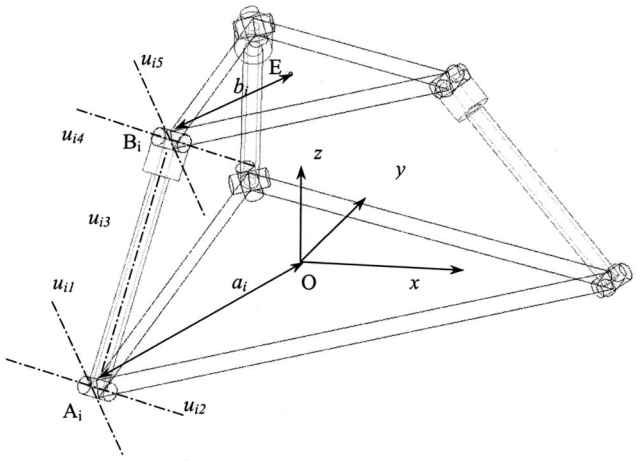

Fig. 4 Joint axes in the 3-UPU platform

$$^{A}\mathbf{e}=[e_x,e_y,e_z]^T \tag{2}$$

For the direct kinematics the leg lengths q_i and the triangular plates' geometry are known and the 3 coordinates of vector $\mathbf{e}$ are determined from the following 3 scalar equations (the dot "·" in this equation represents the dot product of two vectors):

$$\mathbf{e}^2-2\mathbf{e}\cdot\mathbf{c}_i+\mathbf{c}_i^2=q_i^2, \quad \text{for } i=1,2,3. \tag{3}$$

For the inverse kinematics vector $\mathbf{e}$ and the triangular plates' geometry are known and the limb lengths, q_i are calculated from the following 3 equations:

$$q_i=\pm\sqrt{(e_x-c_{ix})^2+(e_y-c_{iy})^2+e_z^2}, \tag{4}$$

The manipulator Jacobian matrix $\mathbf{J}$ relates the end-effector velocities vector $\dot{\mathbf{x}}$ to the actuated joint velocities vector $\dot{\mathbf{q}}$:

$$\dot{\mathbf{q}}=\mathbf{J}\dot{\mathbf{x}} \tag{5}$$

For the 3-UPU platform $\mathbf{J}$ is a 3×3 matrix and is given by Eq. (6). (Note: in this paper we did not consider the rotation Jacobian and so the workspace may not be free of rotation singularities. These constraints are considered in the following references [10,17,18]).

$$\mathbf{J}=[\mathbf{u}_{1,3}^T \quad \mathbf{u}_{2,3}^T \quad \mathbf{u}_{3,3}^T]^T \tag{6}$$

The condition number of the Jacobian matrix is defined by Eq. (7):

$$k=\|\mathbf{J}\|\cdot\|\mathbf{J}^{-1}\| \tag{7}$$

where the dot "·" in this equation represents the multiplication of two scalars, and $\|\cdot\|$ denotes the norm 2 of a matrix [19].

Robot manipulators and their configurations where *k* is equal to 1 are called isotropic. In these configurations the system is able to develop same amount of forces and velocities in all end-effector directions. For high values of *k*, there are end-effector directions where the manipulator can develop much higher forces or velocities than in other directions. In many applications, this is not a desirable system property because the system looses its homogeneity in force and velocity development. Configurations in which *k* has an infinite value are singular configurations. In these configurations there are directions in space where the end-effector can either not move or not apply forces. Isotropy is a very local manipulator property because it changes from configuration to configuration. A manipulator can have a good isotropy in one configuration and a bad one in another. In many robot applications

isotropy is an important property, and needs to be taken into account during the robot's design phase. Defining a global isotropy index that will be able to characterize the system isotropy in the whole workspace is an important but difficult problem to solve. The problem is that a robot system will always have singular or bad isotropy configurations. By taking a type of an average of the condition number is only a rough indication of the quality of the system global isotropy and says nothing about the magnitude and number of bad isotropy configurations. Nevertheless, in this work we will use global isotropy indices based on the average of the condition number, as they are being used in the current literature.

In this work, three performance indices will be used to characterize a robotic system's workspace as it is described in detail in Sec. 3:

a) The workspace volume. Obviously, using this performance index as the objective function, optimal designs correspond to maximum workspace volume.

b) The average of the inverse of the condition number. The condition number characterizes the system's isotropy. The average of the inverse of the condition number is calculated by summing the inverse of the condition number in every point in the workspace and then dividing it with the number of points considered in the workspace. Optimal designs correspond to values of the average of the inverse of the condition number close to 1.

c) The Global Condition Index as it is used in [9]. An initial definition of a Global Performance Index was proposed in [20]. This index, defined in Eq. (8), is the ratio of the integral of the inverse condition numbers calculated in the whole workspace, divided by the volume of the workspace:

$$\eta_{GA}=\frac{A}{B}, \quad \text{where } A=\int_W\left(\frac{1}{k}\right)dW, \text{ and } B=\int_W dW, \quad (8)$$

in which k is the condition number at a particular point in the workspace W. B is the total volume of the workspace. The Global Condition Index is bounded as:

$$0<\eta_{GA}<1 \quad (9)$$

Isotropic systems correspond to value of η_{GA} equal to 1 and systems with bad isotropy correspond to values of η_{GA} approaching zero.

The Global Condition Index used in this paper is given in Eq. (10) and consists only of the numerator of the index defined in Eq. (8). In reality it is calculated as the product of the average of the inverse condition number with the workspace volume. Therefore, it is like a combination of the first two performance indices.

$$\eta=\int_W\left(\frac{1}{k}\right)dW \quad (10)$$

where W and k have the same meaning as in Equation (8).

2.2 3-UPS Orientational Platform. The 3-UPS parallel platform consists of a fixed tetrahedron, a moving tetrahedron and three identical limbs (see Fig. 3). The tetrahedrons have equilateral triangular bases of different sizes. The tips of the tetrahedrons are connected using a spherical joint. The limbs are connected to the moving tetrahedron base with 2-DOF universal joints and to the fixed tetrahedron base with spherical joints. A linear actuator controls the leg length, and forms a prismatic joint. Each universal joint is treated as two revolute joints with axes perpendicular to each other and intersecting at a point. In Fig. 5, u_{i4} is the unit vector along the prismatic joint axis for leg i, u_{i5} and u_{i6} are the unit vectors along the axes of the universal joint of leg i. u_{i7} is the CB_i edge of the moving tetrahedron.

A coordinate system is chosen for each tetrahedron as shown in Fig. 6, a) and b). Frames A and B are defined for the base and moving tetrahedrons respectively. Their origin is placed at the common tip of the tetrahedrons and represents the point around which the moving tetrahedron rotates. Their z-axis is perpendicular to each base triangle's plane, and their x and y-axes are in planes parallel to the base triangle's plane. The $x_{a/b}$ axes are oriented parallel to the OA_1 and EB_1 lines, respectively. The frame A, $Cx_ay_az_a$, is rigidly connected to the fixed tetrahedron and has

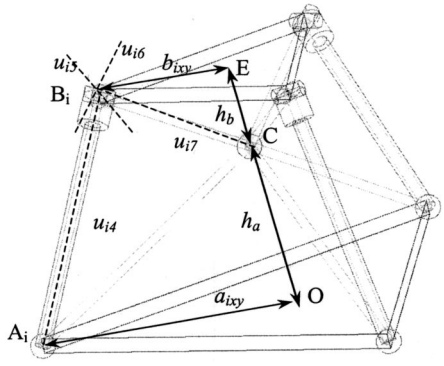

Fig. 5 Joint axes in the 3-UPS platform

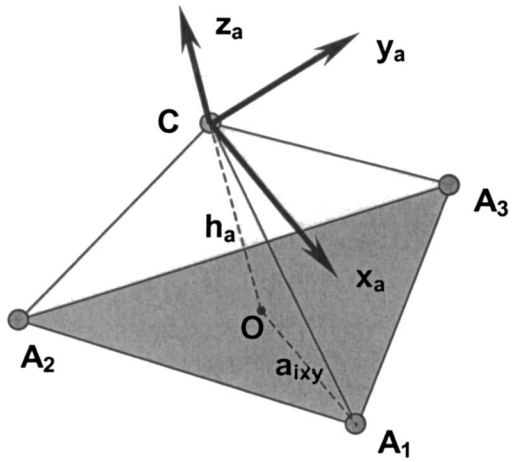

a) Base Tetrahedron

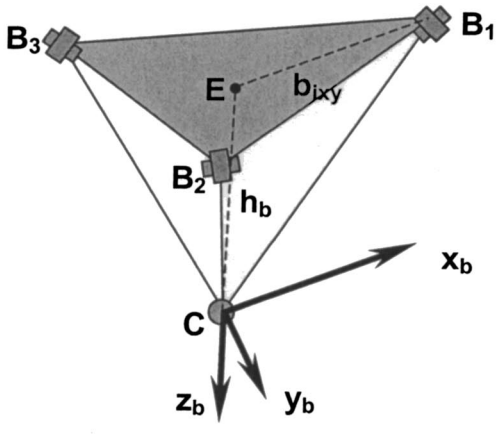

b) Moving Tetrahedron

Fig. 6 Coordinate systems of the 3-UPS platform

center C at the tetrahedron's tip. The point O is the center of the base triangle. The z_a axis is oriented along OC. The x_a axis is parallel to OA_1 and the y_a axis is chosen to obtain a right hand rectangular coordinate system. The frame B, $Cx_by_bz_b$, is rigidly connected to the moving tetrahedron and has the same center as the fixed frame, A. The point E is the center of the base triangle of the moving tetrahedron. The z_b axis is oriented along the vector EC. The x_b axis is parallel to the EB_1 and y_b axis is chosen to obtain a right hand rectangular coordinate system.

As seen in Fig. 6, the position vectors of points A_i and B_i with respect to frames A and B respectively, can be written as:

$$ {}^A\mathbf{a}_i=[a_{ix},a_{iy},-h_a]^T, \quad \text{and} \quad {}^B\mathbf{b}_i=[b_{ix},b_{iy},-h_b]^T \tag{11}$$

The scalar a_{ixy} (shown in Fig. 6) denotes the distance between the center, O, of the base triangle of the fixed tetrahedron and anyone of the corners of the base triangle. The scalar b_{ixy} denotes the distance between the center, E, of the base triangle of the moving tetrahedron and any of the corners of the base triangle. The parameter c_i denotes the difference between a_{ixy} and b_{ixy}.

Parameter d_i denotes the length of leg i. The vector $\mathbf{d}_i$ represents the position vector of the leg i (A_iB_i) in the base coordinate system:

$$ {}^A\mathbf{d}_i=[d_{i,xa},d_{i,ya},d_{i,za}]^T \tag{12}$$

The scalar h_a denotes the height of the fixed tetrahedron and is the distance from point O to point C. The scalar h_b denotes the height of the moving tetrahedron and is the distance from point E to point C. The parameter h represents the total height of the parallel platform in (0,0,0) orientation and is equal to the sum of h_a and h_b. The parameter h_{ab} is the ratio between h_a and h_b.

The transformation from the moving frame B to the fixed frame A can be described by a 3×3 rotation matrix ${}^AR_B$ defined by a z-x-z (φ-θ-ψ) Euler rotation. Given that in the initial position (0-0-0 rotation) the x_a and x_b axes coincide, z_a and z_b, and y_a and y_b are in opposite directions respectively, the resulting rotation matrix is given by:

$$ {}^AR_B=\begin{bmatrix} c\phi c\psi-s\phi c\theta s\psi & c\phi s\psi+s\phi c\theta c\psi & -s\phi s\theta \\ s\phi c\psi+c\phi c\theta s\psi & s\phi s\psi-c\phi c\theta c\psi & c\phi s\theta \\ s\theta s\psi & -s\theta c\psi & -c\theta \end{bmatrix} \tag{13}$$

where c represents the cosine and s the sine of the following angle.

For the direct kinematics the leg lengths d_i and the triangular bases' geometry are known. The three orientation angles of the moving platform are determined from expanding the following three scalar equations (see [2] for more details):

$$ d_i^2=\mathbf{a}_i^2+\mathbf{b}_i^2-2\mathbf{a}_i^T\mathbf{b}_i, \quad \text{for } i=1,2,3 \tag{14}$$

For the inverse kinematics the orientation of the moving platform is known and the limb lengths, d_i are calculated from the following three equations:

$$ d_i=\pm\sqrt{\mathbf{a}_i^2+\mathbf{b}_i^2-2\mathbf{a}_i^T\mathbf{b}_i}, \quad \text{for } i=1,2,3 \tag{15}$$

The manipulator Jacobian matrix $\mathbf{J}$ relates the end-effector velocities vector ω to the actuated joint velocities vector $\dot{\mathbf{d}}$:

$$ \mathbf{J}_x\boldsymbol{\omega}+\mathbf{J}_d\dot{\mathbf{d}}, \quad \mathbf{J}=\mathbf{J}_d^{-1}\mathbf{J}_x \tag{16}$$

For the 3-UPS platform $\mathbf{J}_x$ and $\mathbf{J}_d$ are given by:

$$ \mathbf{J}_x=\begin{bmatrix} (\mathbf{u}_{1,7}\times\mathbf{u}_{1,4})^T \\ (\mathbf{u}_{2,7}\times\mathbf{u}_{2,4})^T \\ (\mathbf{u}_{3,7}\times\mathbf{u}_{3,4})^T \end{bmatrix} \quad \mathbf{J}_d=[I] \tag{17}$$

The condition number of the Jacobian matrix is defined by Eq. (18)

$$ k=\|\mathbf{J}\|\cdot\|\mathbf{J}^{-1}\| \tag{18}$$

where $\|\cdot\|$ denotes the norm 2 of a matrix [19].

The same three performance indices as for the 3-UPU platform are used to characterize the platform's workspace.

3 Optimization Algorithms

3.1 3-UPU Translational Platform. Based on the direct kinematics of the 3-UPU parallel platform, shown in Eq. (3), the platform's workspace depends on two geometric parameters: the magnitude c_i of vector $\mathbf{c_i}$ and the stroke s_i of the prismatic joint which is directly related to each leg's length q_i. Due to the fact that the 3-UPU platforms have equilateral triangular base and moving plates, and assuming that all legs are using the same actuator, then c_i and s_i have the same value for all legs.

The stroke s_i of the actuator is the maximum amount of travel for each leg's prismatic actuator. It is expressed with a percentage value of the minimum length of the limb $q_{\min}$, which in turn is taken such that $q_{\max}$ is equal to 1. The fact that the leg's maximum length is considered to be equal to 1 means that all lengths are normalized with respect to the leg's maximum length as it is specified from each application's requirements. In this project the range of values of the stroke of the actuators is considered to be between 20% and 87.5%. These values were selected based on the technical specifications of the majority of commercially available prismatic actuators. The minimum value of each leg's length $q_{\min}$ is equal to $1/(1+s_i/100)$. So in each platform's configuration the value of the leg length q_i should be between $q_{\min}$ and 1.

The range of values for c_i is between 0.27 and 0.645. Platforms with values for c_i close to zero (i.e., platforms where the triangular base and moving plates are almost equal) present extra DOF (self-motions) that could not be controlled from the actuation motion and such designs are not acceptable. Platforms with very large values for c_i have very small workspace.

The algorithm to calculate the platform's workspace as a function of the design parameters consists of the following steps:

a) The algorithm selects the values of c_i and s_i from their acceptable ranges of values. For s_i, 27 values in equal increments are selected between 20% and 87.5%. For c_i, 15 values in equal increments are selected between 0.27 and 0.645.

b) A three-dimensional, rectangular shaped enclosure box is determined that includes all points that can be reached by the center of the moving plate. Usually, this box is selected larger than the expected platform's workspace to be sure that all points in the platform's workspace are included in the enclosure box. For each set of values of c_i and s_i a Monte Carlo method is used to randomly select 1,000,000 points inside the determined enclosure box.

c) For each selected point, the platform's inverse kinematics is solved using Eq. (4). In order that the selected enclosure point lies in the platform's unconstrained workspace, the calculated length q_i should be a real number and lie in the range from 0 to 1. If in addition the determined limb length q_i is within the acceptable range of motion of the actuator, i.e., between $q_{\min}$ and 1, then the selected enclosure point is within the actuator-constrained workspace.

d) Using Eq. (7), the condition number k is calculated at each enclosure point found to be within the platform's unconstrained workspace.

e) Once the condition number of all points in the unconstrained workspace has been calculated then the three performance indices are calculated. The workspace volume is determined by multiplying the volume of the enclosure box with the total number of

points inside the workspace and dividing it by the total number of points generated. The average of the inverse of the condition number is calculated by dividing the sum of the reciprocal of the condition numbers with the total number of points inside the workspace. The Global Condition Index is determined from Eq. (10). Is calculated as the product of the sum of the reciprocal of the condition numbers with the volume of the unconstrained workspace and divided by the total number of points inside the workspace.

f) For each point within the constrained workspace the angles of the revolute joints (each universal joint is treated as two revolute joints) at the base are determined using inverse kinematic equations. If all of them fall between the allowable angular limits, then the point is within the joint-constrained workspace. The angular limits of the revolute joints were chosen such that the condition number of the platform remains below 10 at every nonsingular configuration.

The unconstrained workspace and the calculation of its global condition number verified the results of [6]. However, the emphasis of this work for the 3-UPU platform is the identification of the properties of the actuator-constrained workspace and of the joint-constrained workspace and our results are presented in Sec. 4.

3.2 3-UPS Orientational Platform. Based on the platform's direct kinematics, and due to the fact that all legs are equal and that the base and moving triangles are equilateral, the 3-UPS orientational platform workspace depends on four geometric parameters: a) the difference c_i between a_{ixy} and b_{ixy}: $c_i = a_{ixy} - b_{ixy}$; b) the total height of the platform considered as the sum of the heights of the two tetrahedra: $h = h_a + h_b$ (see Fig. 5); c) the ratio of the heights of the two tetrahedra: $h_{ab} = h_a / h_b$; and d) the stroke of the prismatic joint s_i.

The range of values for c_i and s_i parameters has been selected in the same way as with the 3-UPU platform. For the other two design parameters we considered the range of possible values as follows. The total height of the two tetrahedrons, h, has values between 0.2 and 1.0. Below 0.2 the workspace is very small and has no practical use. Total height equal to 1 corresponds to maximum length. The ratio of the heights of the two tetrahedrons, h_{ab}, was selected to vary between 0.33 and 3.0.

Due to the fact that the plots of all three performance indices for any value of the design parameters are highly non-monotone, a Genetic Algorithm was implemented to determine the optimal design configuration. It consists of the following steps:

a) An initial population of 100 members is randomly generated. Each member contains values for the four design parameters defined above. Each parameter has an eight digit resolution which means that 256 different values can be chosen for each parameter.

b) For each population member the platform's geometric parameters are calculated using the design parameters.

c) To determine the values of the performance indices a Monte Carlo method was implemented. For each configuration with certain values of the design parameters, s_i, c_i, h, and h_{ab}, 1,728,000 orientations of the moving tetrahedron are chosen randomly. The φ, θ and ψ Euler angles corresponding to a z-x-z rotation are randomly chosen in the interval $[-180$ deg, $+180$ deg$]$.

d) For each orientation the lengths of the legs are determined using the inverse kinematics, Eq. (15). If all legs have lengths in the allowed interval $d_{\min} < d < d_{\max}$ the interference of the legs with fixed and moving tetrahedrons is checked. Also, for the constrained workspace, the joint angles are determined and verified if they are between imposed limits. Additionally, the interference of one leg with another and the interference of each leg with the central spherical joint are verified. If the orientation verifies all constraints, then the Jacobian condition number, k, is determined using Eq. (18).

e) For each configuration the performance indices are calculated using Eq. (10). The population member with the best objective function is determined and saved in a file. It will be called "the king" in further references. Any one of the described performance indices can be chosen as the objective function.

f) A mating pool is then created from the initial population selecting the members with better objective function values. The first member of the mating pool is chosen as the member with the best value of the objective function (the king).

g) A crossover among the members of the mating pool is done with a 0.45 probability. At the end, the first member is replaced with the member with the best objective function (the king).

h) A mutation with 0.05 probability is then done over the new population. The first member of the population is not affected (the king).

i) For the new population the cycle starts over. It stops when the value of the objective function of the king is not improved with a certain relative quantity.

The unconstrained optimization is done without imposing the constraints mentioned in step d) above.

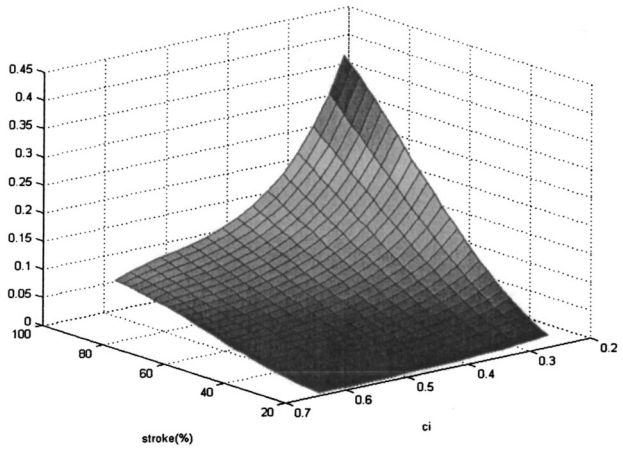

Fig. 7 Workspace volume of the 3-UPU platform

4 Results

4.1 3-UPU Translational Platform. Figure 7 shows the volume of the constrained workspace as a function of the actuator stroke, $s_i(\%)$, and the design parameter, c_i. Dark red points indicate a large value of the volume while dark blue indicate a small value. From the plot it can be seen that the volume of the constrained workspace increases as the stroke increases and as the value of the c_i parameter decreases.

Figure 8 shows the average value of the inverse of the condition number as a function of $s_i(\%)$ and of c_i. It can be seen that isotropy is affected a lot by c_i. Isotropic designs correspond to platforms with large values of c_i. In these platforms the moving plate is much smaller than the base. Such platforms do not present self-motions (i.e., extra uncontrollable DOF) as those platforms with very small c_i do. Hence, these designs are away from singular designs and hence they present good isotropic behavior. Generally, the stroke does not affect isotropy as seen from Fig. 8. However, for large values of c_i, where in general isotropy is very good, the best designs correspond to strokes between 30% and 40%.

Figure 9 shows the Global Condition Index as a function of the design parameters. Overall, the Global Condition Index increases as stroke increases. So if good isotropy, within the whole workspace, is desired combined with large workspace volume, then actuators with high strokes should be used. For these large stroke values the Global Condition Index shows a maximum for values of the design parameter c_i around 0.55 and around 0.27. These can be considered as optimal design values for c_i if the Global Condition Index is used as the design criterion.

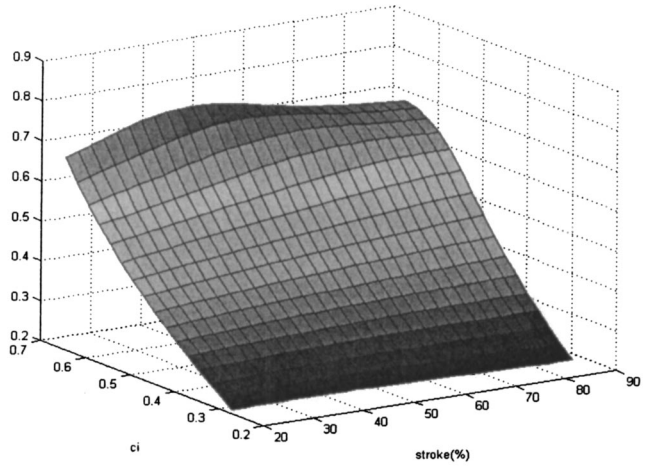

Fig. 8 Average of the inverse of the condition number of the 3-UPU platform

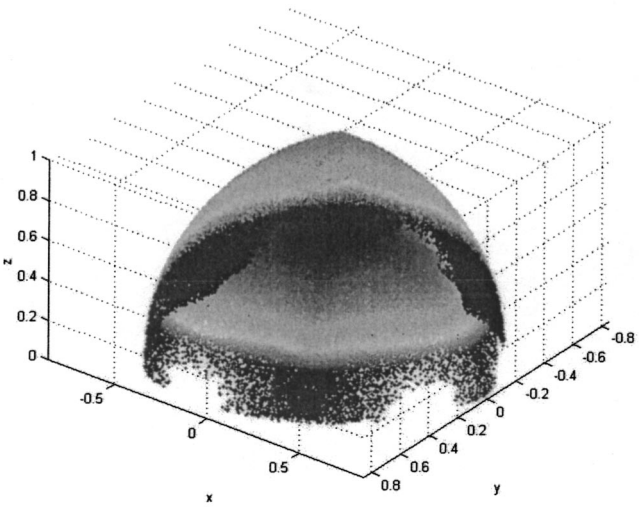

Fig. 10 Workspace without angular constraints (c_i=0.27 and s_i=85%) of the 3-UPU platform

The role of angular constraints for universal joints is to include the practical limits of the universal joints and to avoid points with high condition number. Figures 10 and 11 present the workspace of the 3-UPU parallel platform for c_i equal to 0.27 and stroke equal to 85% without and with angular constraints, respectively. These values of stroke and of *ci* are the optimal ones based on the Global Condition Index shown in Fig. 9. The color of the points reflects the value of the condition number. The dark blue points have small condition numbers and they are generally found toward the center of the workspace. The dark red points have high condition numbers and they are generally found toward the bottom edges of the workspace. It can clearly be seen that by imposing stricter constraints on the range of motion of the universal joints, the workspace isotropy is improved while the workspace volume is slightly decreased.

4.2 3-UPS Orientational Platform. We used a program written in C++ to perform the optimization and MATLAB™ to plot the workspace. We run the optimization program for the constrained and unconstrained workspace.

The optimal design for the unconstrained workspace has the following parameter values: stroke=83.9%, c_i=0.602, h =0.285, and h_{ab}=0.344. Figure 12 shows the workspace of the optimal unconstrained configuration. The points represent the positions that can be reached by the center, *E*, of the moving tetrahedron base. *E* describes a sphere with the center at point *C* and a radius h_b. To represent the twist angle, ψ, the radius of the sphere described by point *E* was changed depending on the value of the twist angle. For $\psi=-180$ deg the radius was reduced by 10% of h_b and for $\psi=+180$ deg it was increased by 10%. A linear dependence was used for the intermediary values. The color with which the points were represented reflects the value of the condition number of the platform's Jacobian at the specific point. A value 1 of the condition number was represented with dark blue color. Because some of the condition numbers had extremely large values (more than 100), in our representation in MATLAB™ all condition numbers with a value over 10 were reduced to 10 (This was used just for representation but not for optimization). Dark red color is used to plot points with large condition numbers.

For the optimization of the constrained workspace, we imposed limits at the universal and spherical joints of the platform. The universal joints were considered as two perpendicular revolute joints with one common point. In this paper we present results from two different schemes of constrained workspaces with and without considering the legs interference.

For the first set of constraints we set the limits of the universal joint angles at ± 75 deg for the revolute joint that allows the leg

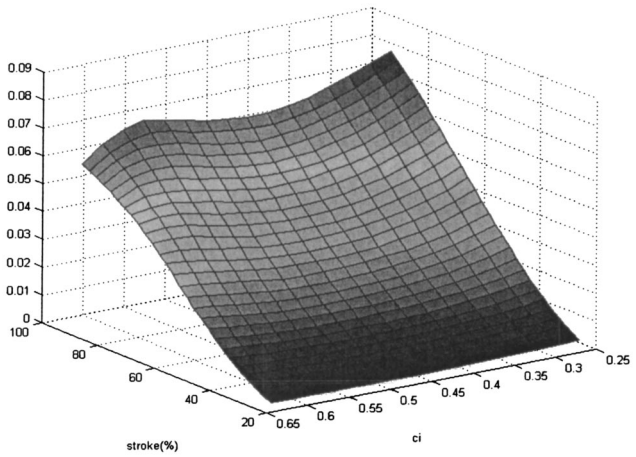

Fig. 9 Global condition index of the 3-UPU platform

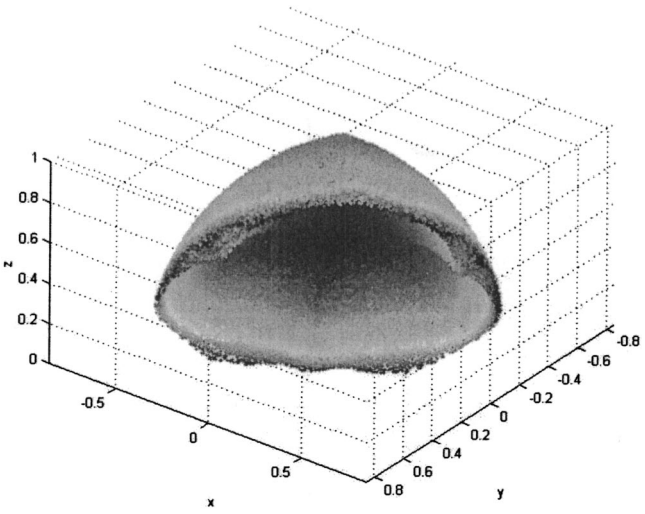

Fig. 11 Workspace with angular constraints (c_i=0.27 and s_i =85%) of the 3-UPU platform

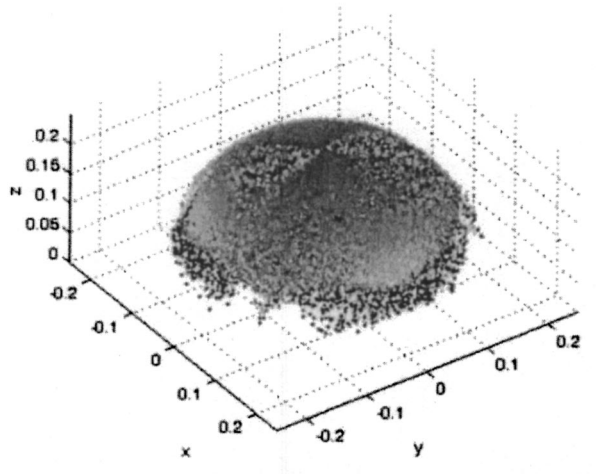

Fig. 12 Workspace of the optimal unconstrained configuration of the 3-UPS platform

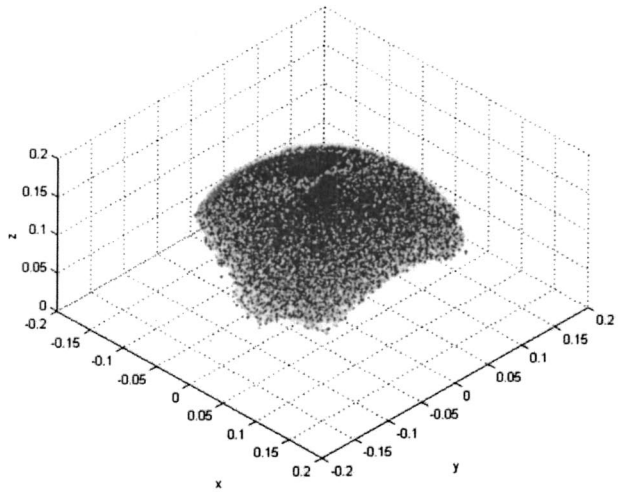

a) First Scheme of Joint Constraints (I)

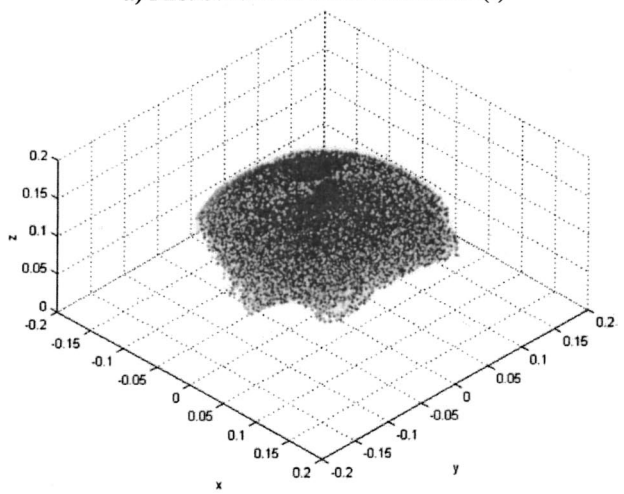

b) Second Scheme of Joint Constraints (II)

Fig. 13 Workspace of the optimal constrained configuration of the 3-UPS platform

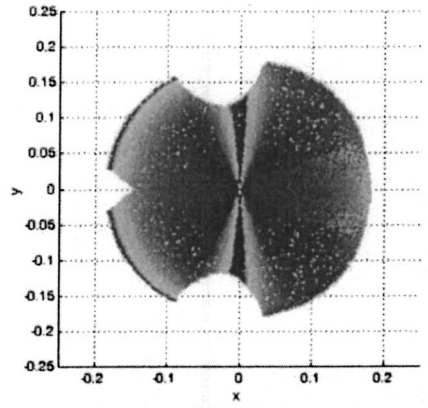

a) – Unconstrained Workspace

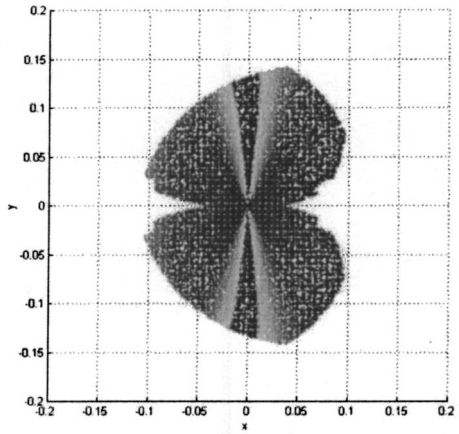

b) – Constrained Workspace (I)

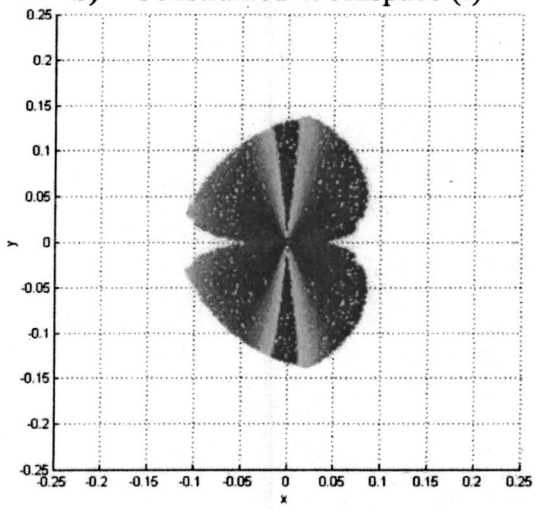

c) – Constrained Workspace (II)

Fig. 14 Top view of the unconstrained and constrained workspaces for fixed twist of 0.0 deg of the 3-UPS platform

rotation on CEB_i planes and ± 85 deg for the other revolute joint. The limits for the spherical joint angles were set the same, at ± 65 deg. The optimal design parameters that were obtained are: stroke $= 71\%$, $c_i = 0.62$, $h = 0.44$ and $h_{ab} = 1.75$. In this case the average value of the inverse of the condition number, k, is increased and the workspace volume is decreased relative to the

unconstrained optimal configuration. The workspace for the optimal 3-UPS platform with the first set of constraints is shown in Fig. 13(*a*).

For the second scheme we considered also constraints due to possible interference of one leg with another and possible interference of each leg with the central spherical joint. We used the same angular limits for the universal and spherical joints. The optimal design parameters that were obtained are: stroke = 70%, $c_i = 0.61$, $h = 0.48$, and $h_{ab} = 2.04$. The workspace for the optimal 3-UPS platform with the second set of constraints is shown in Fig. 13(*b*).

For the constrained workspaces we used the same representation method as for the unconstrained workspace. From the data provided by the optimization programs, it can be seen that the constrained workspace volume is less than half the unconstrained workspace volume. By imposing constraints on the joint angles, one can exclude not only many bad isotropy points, but many good isotropy points as well. Overall, the average value of the inverse of the condition number is increased, which means that the isotropy of the platform is improved, and the workspace volume is reduced when joint constraints are imposed. It can also be seen that the joint constraints did not affect significantly the optimal value for the design parameter c_i . This means that for a better design, the difference in size between the bases of the tetrahedrons needs to be very large, independently of the joint constraints imposed.

Figures 14 and 15 present the top view of the unconstrained and constrained workspaces for 0 deg and 30 deg twist angles, respectively. Here the effect of the workspace reduction due to the angular constraints is more obvious. Even though the workspaces shown in Fig. 12–15 are continuous, not all of the points can be reached with any orientation. This is shown in Fig. 14(*b*), (*c*) and 15(*b*), (*c*). Also it can be seen that for small values of the pitch angle, φ, the manipulator has a bad isotropy, no matter how small the yaw angle, θ, or the twist angle, ψ, are.

From Figs. 13, 14, and 15 we learn that points on the workspace can be reached only for certain twist angles. Also we learn that even though some points can be reached for a large range of twist angles for some values of these we get a better isotropy. These results can be used to determine a path between two orientations maintaining a good isotropy if the twist angle in the intermediate positions is not critical.

5 Conclusions

In this paper the workspace optimization of two types of 3-legged parallel platforms is performed. The platforms are the 3-UPU with only translational DOF and the 3-UPS with only rotational DOF. Both platforms are considered to be used as joint modules in reconfigurable robots and the quality of their constrained workspace is an important design feature.

For the 3-UPU platform the workspace is parameterized using two design parameters, which are the prismatic joint stroke and the difference between the distances of the center to one of the corners of the triangular plate of the base and of the moving platform. Three workspace performance indices are calculated as a function of the design parameters and optimal solutions for these design parameters are determined. These performance indices quantify the workspace volume, the system isotropy and a combination of the two properties. It is shown that for different performance indices different parameters correspond to the best design. The limits that the actual actuators and joints impose determine limitations in the workspace of parallel platforms but they can be used in the same time to exclude points with bad isotropy from the platform's workspace. For the 3-UPS platform the workspace is parameterized using four design parameters. In the same way as with the 3-UPU, three workspace performance indices are calculated as a function of the design parameters. The optimal design is determined for the unconstrained and constrained situations. For the constrained workspace both situations with and without legs interference are considered. Different design parameters are obtained in the three situations. The paper presents the total and fixed twist unconstrained and constrained workspaces.

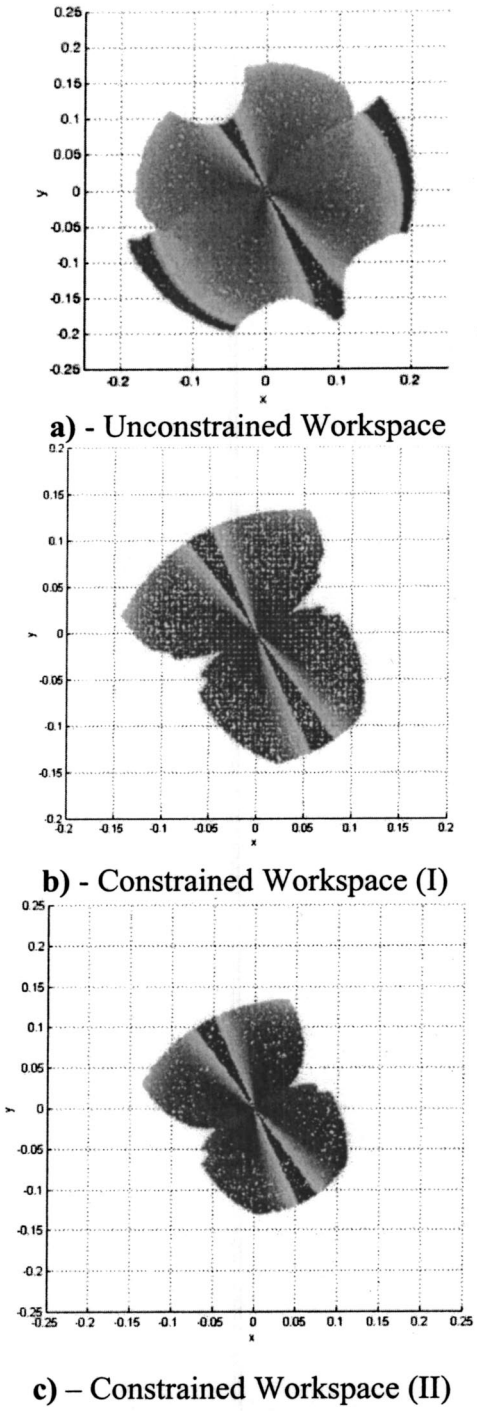

Fig. 15 Top view of the unconstrained and constrained workspaces for fixed twist of 30 deg of the 3-UPS platform

Acknowledgments

This work was supported by a National Science Foundation CAREER Award (DMI-9984051). Additional support was provided by a Rutgers University Research Council Grant and by NASA's Jet Propulsion Laboratory.

References

[1] McKee, G., and Schenker, P., Ed., 1999, *Sensor Fusion and Decentralized Control in Robotic Systems II*, SPIE Proceedings Series, Vol. 3839.

[2] Tsai, L.-W., 1999, ''Robot Analysis—The Mechanics of Serial and Parallel Manipulators,'' John Wiley & Sons, New York.

[3] Merlet, J.-P., 2000, *Parallel Robots*, Kluwer, Dordrecht, Netherlands.

[4] Hamlin, G., and Sanderson, A., 1997, ''TETROBOT: A Modular Approach to Parallel Robotics,'' IEEE Rob. & Autom. Mag., **4**(1), pp. 42–49.

[5] Tsai, L.-W., and Joshi, S., 2001, ''Feasibility Study of Hybrid Kinematis Machines,'' *Proceedings of the 2001 NSF Design, Manufacturing and Industrial Innovation Research Conference*, Tampa, FL, January 7–10.

[6] Tsai, L.-W., 1996, ''Kinematics of a Three-DOF Platform with Three Extensible Limbs,'' *Recent Advances in Robot Kinematics*, Lenarcic, J. and Parenti-Castelli, V., eds., Kluwer Academic Publishers, pp. 401–410.

[7] Di Gregorio, R., and Parenti-Castelli, V., 1998, ''A Translational 3-DOF Parallel Manipulator,'' *Advances in Robot Kinematic: Analysis and Control*, J. Lenarcic and M. L. Husty, eds., Kluwer Academic Publishers, pp. 49–58.

[8] Di Gregorio, R., and Parenti-Castelli, V., 1999, ''Mobility Analysis of the 3-UPU Parallel Mechanism Assembled for a Pure Translational Motion,'' *Proceedings of the 1999 IEEE/ASME International Conference on Advanced Intelligent Mechatronics*, AIM'99, Atlanta, Georgia, September 19–23, pp. 520–525.

[9] Tsai, L.-W., and Joshi, S., 2000, ''Kinematics and Optimization of a Spatial 3-UPU Parallel Manipulator,'' ASME J. Mech. Des., **122**(4), pp. 439–446.

[10] Parenti-Castelli, V., Di Gregorio, R., and Bubani, F., 2000, ''Workspace and Optimal Design of a Pure Translation Parallel Manipulator,'' Meccanica, **35**, pp. 203–214, Kluwer Academic Publishers.

[11] Merlet, J. P., 1999, ''Determination of 6D Workspace of Gough-Type Parallel Manipulator and Comparison between Different Geometries,'' Int. J. Robot. Res., **18**(9), September, pp. 902–916.

[12] Tsai, L.-W., 1999, ''Systematic Enumeration of Parallel Manipulators,'' *Parallel Kinematic Machines: Theoretical Aspects and Industrial Requirements*, C. R. Boer, L. Molinari-Tosatti, and K. S. Smith, eds., Advanced Manufacturing Series, Springer-Verlag, ISBN: 1-852-33613-7, pp. 33–49.

[13] Gosselin, C., and Hamel, J., 1994, ''The Agile Eye: A High-Performance Three-Degree-of-Freedom Camera-Orienting Device,'' *Proceedings IEEE International Conference on Advanced Robotics*, Pisa, Italy, pp. 781–786.

[14] Ouerfelli, M., and Kumar, V., 1991, ''Optimization of a Spherical Five Bar Parallel Drive Linkage,'' *DE, Advances in Design Automation*, Vol. 1, pp. 171–177.

[15] Gosselin, C., and Angeles, J., 1989, ''The Optimum Kinematic Design of a Spherical Three-Degree-of-Freedom Parallel Manipulator,'' ASME J. Mech. Transm., Autom. Des., **111**(2), pp. 202–207.

[16] Joshi, S. A., 2002, ''Comparison Study of a Class of 3-DOF Parallel Manipulators,'' Ph.D. Dissertation, University of Maryland, College Park, May.

[17] Zlatanov, D., Bonev, I., and Gosselin, C., 2001, ''Constraint Singularities,'' Newsletter on http://www.parallelmic.org, July.

[18] Joshi, S. A., and Tsai, L.-W., 2002, ''Jacobian Analysis of Limited-DOF Parallel Manipulators,'' Trans. ASME, **124**, June, pp. 254–258.

[19] Chapra, S., and Canale, R., 1998, *Numerical Methods for Engineers: With Programming and Software Applications*, WCB/McGraw-Hill.

[20] Gosselin, C., and Angeles, J., 1991, ''A Global Performance Index for the Kinematic Optimization of Robotic Manipulators,'' ASME J. Mech. Des., **113**(3), pp. 220–226.